Chinese Journal of Aeronautics, (2023), 36(7): 25–39

Chinese Society of Aeronautics and Astronautics
& Beihang University

Chinese Journal of Aeronautics

cja@buaa.edu.cn
www.sciencedirect.com

Modelling of grinding mechanics: A review

Qingyu MENG [a], Bing GUO [a,*], Qingliang ZHAO [a], Hao Nan LI [b], Mark J. JACKSON [c], Barbara S. LINKE [d], Xichun LUO [e]

[a] *Center for Precision Engineering, School of Mechatronics Engineering, Harbin Institute of Technology, Harbin 150001, China*
[b] *School of Aerospace, The University of Nottingham Ningbo, Ningbo 315100, China*
[c] *School of Integrated Studies, College of Technology and Aviation, Kansas State University, Salina, KS 67401, USA*
[d] *Department of Mechanical and Aerospace Engineering, University of California Davis, Davis, USA*
[e] *Centre for Precision Manufacturing, DMEM, University of Strathclyde, Glasgow, UK*

Received 23 July 2022; revised 10 August 2022; accepted 13 September 2022
Available online 27 October 2022

KEYWORDS

Force modeling;
Grinding;
Grinding mechanics;
Macro force;
Micro force;
Model application

Abstract Grinding is one of the most widely used material removal methods at the end of many process chains. Grinding force is related to almost all grinding parameters, which has a great influence on material removal rate, dimensional and shape accuracy, surface and subsurface integrity, thermodynamics, dynamics, wheel durability, and machining system deformation. Considering that grinding force is related to almost all grinding parameters, grinding force can be used to detect grinding wheel wear, energy calculation, chatter suppression, force control and grinding process simulation. Accurate prediction of grinding forces is important for optimizing grinding parameters and the structure of grinding machines and fixtures. Although there are substantial research papers on grinding mechanics, a comprehensive review on the modeling of grinding mechanics is still absent from the literature. To fill this gap, this work reviews and introduces theoretical methods and applications of mechanics in grinding from the aspects of modeling principles, limitations and possible future trendencies.

1. Introduction

Machining mechanics is the physical link between tools and workpiece, inherently leading to effective material removal in machining. For precision machining processes such as grinding, the importance of machining mechanics may be even more obvious. Grinding force strongly affects material removal rate, dimensional and shape accuracy, surface and subsurface integrity, grinding thermodynamics, dynamics, wheel durability, and machining system deformation.[1–11] Considering that grinding force is related to almost all grinding parameters, grinding force can be used to detect grinding wheel wear, energy calculation, chatter suppression, force control and grinding process simulation. With the grinding force, the machining parameters and the structure of the grinding machine and fixture can be optimized to fully exploit the potential of the grinding process. Substantial academic and engineering efforts have been paid so far to understand grind-

* Corresponding author.
E-mail address: guobing@hit.edu.cn (B. GUO).

Peer review under responsibility of Editorial Committee of CJA.

Production and hosting by Elsevier

https://doi.org/10.1016/j.cja.2022.10.006

ing mechanics with the special focus on force modelling because of the difficulties in experimental observation or measurement. This increasing importance of grinding mechanics can be clearly identified by the annual publication since 1990. As seen in Fig. 1, the statistical results are obtained by searching titles, abstracts and keywords related to grinding force in web of science core database, and all types of references are considered in the Science Citation Index Expanded. An increasing number of research work on grinding force have been publishing, among which the proportion of grinding force model has been also rising. The existing empirical force models seem no longer meet the academic need, and more advanced grinding mechanics models need to be continuously developed.

In spite of the important role, one might be surprised that a comprehensive review of grinding mechanics modeling is still absent from literature, although grinding tools,[12,13] kinematics,[14–16] coolants,[17–19] even grinders[20–22] have been well documents, reviewed and published.

To fill this gap, the present progress of grinding force modeling is reviewed and critically discussed in this work. According to whether abrasive level details is considered, the grinding force modeling can be divided into macro and micro grinding force modeling in Section 2 (see Fig. 2). Macro grinding force focuses on the integrated modeling of grinding wheel dimensions, considering the input of average and experimental parameters. Micro grinding force modeling is based on the interaction between active abrasive grains and workpiece, focusing on the randomness and difference caused by abrasive grains. And in Section 3 and Section 4, the modeling processes of macro and micro grinding force are discussed based on wheel-workpiece interaction and grain-workpiece interaction, respectively. Subsequently, the applications of grinding force modeling are explained in Section 5. Finally, the conclusions and future works are separately summarized in Section 6 and Section 7.

2. Classification of grinding force models

2.1. Macro grinding force model

The macro grinding force model takes the grinding wheel as a whole and is based on average parameters and force coefficients in grinding process.

Average parameter refers to average value of macro process physical quantity, and its essence is related to average chip thickness in grinding process. Back in 1950, Salje[23] proposed a model for the tangential grinding force based on the shear strength of the workpiece material, depth of cut, and width of cut. Based on this, other process parameters[24] such as

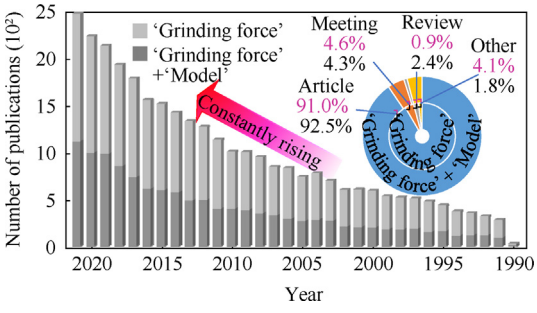

Fig. 1 Annual publication of grinding force since 1990.

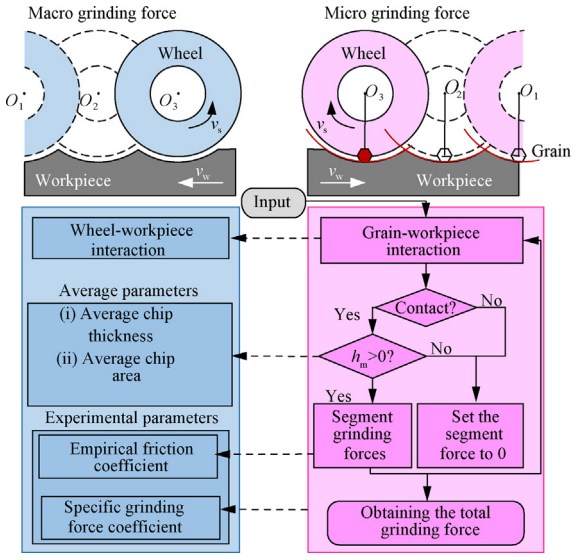

Fig. 2 Classification of grinding force models.

equivalent grinding wheel diameter,[25] grinding wheel speed[26] and workpiece feed speed[27] are also taken into account. In general, although average parameter has the advantages of fast modeling speed and few input parameters, it doesn't take into account difference between grinding forces of abrasive grains.

The second characteristic of macro grinding force model is force coefficient, which is generally calibrated by experiments. Chiu and Malkin[28] carried out sliding experiments in classical physics, and fitted and calibrated the force coefficient by measuring downforce and friction resistance. According to the calibrated force coefficient, Salje[23], Werner and Konig[29] established the normal force and tangential force as multiplication relation. However, these models are based on the premise of invariable workpiece material, abrasive grain size, grinding speed and coolant. A large number of experiments show that the change of sliding force coefficient with the grinding speed largely depends on the coupling of the materials of the tool and the workpiece, and the force properties of different materials are different. For example, the sliding force coefficient of modern ceramic tools increases with the increase of grinding speed,[30] while the sliding force coefficient of cemented carbide tools shows a downward trend.[31] The empirical parameters can be quickly applied to the modeling of chip thickness and grinding force, but they need a lot of calibration experiments to support them, and the particularity cannot be ignored.

Due to the lack of consideration of abrasive grain level in average parameters and experimental parameters, the expression of macro grinding force still cannot analyze the randomness and complexity of grinding process. Macro grinding force model is mostly used for production practice and phenomenon description, and has the characteristics of high efficiency. However, a lot of calibration experiments are needed for different processing conditions to improve the accuracy of fitting coefficient.

2.2. Micro grinding force model

Micro grinding force model is based on the abrasive grain kinematics, and its essence is related to the instantaneous chip thickness caused by a single abrasive grain during grinding.

Abrasive grain kinematics needs to consider the randomness of abrasive grains: the change of the position and geometry of abrasive grains will directly affect the trajectory of abrasive grains.[32] In order to make the abrasive grain model fully represent the real probability property of grinding process, the statistical algorithm is applied. Logarithmic distribution function,[33] Rayleigh probability density function[34] and so on are considered to be the corresponding laws between the density of abrasive grains and chip thickness. However, the statistical results are restricted by many factors, such as statistical samples, grinding conditions, wear conditions and workpiece materials, so they are only suitable for specific grinding conditions. When the heights of active abrasive grains are reduced to the same as that of inactive abrasive grains, the probability distribution rule of abrasive grain height statistics will no longer be applicable[35].

In addition to the randomness of abrasive grains themselves, grinding conditions will also have an impact on the kinematics of abrasive grains. Jamshidi and Budak[36] considered the vibration of abrasive grains caused by the eccentricity of grinding wheel, and the dynamic chip thickness of adjacent active abrasive grains could be obtained. However, the model still uses the concept of average parameter: dividing the average force of revolutions per shaft by the number of effective abrasive grains as the instantaneous grinding force of a single abrasive grain. The surface of abrasive grains with random shapes becomes dull due to abrasive grain wear, dressing or adhesion of metal chips during grinding, which leads to inevitable contact friction phenomena.[37] The contact friction model, as one of the important factors of the micro grinding force model, also needs to be paid attention to.

Micro grinding force model focuses on the level of abrasive grains, which is an effective means to explain the transient change of grinding process. However, the improvement of model accuracy also means that a large amount of data and situations need to be considered, which often takes a lot of time.

3. Modeling process of macro grinding force

The modeling process of most macro grinding force can be summarized as Fig. 3. It is necessary to consider the interaction between grinding wheel and workpiece (Section 3.1) in different grinding modes (Section 3.4). The macro grinding force (Section 3.3) can be obtained by calculating the average undeformed chip thickness (Section 3.2).

3.1. Modeling of the wheel-workpiece interaction

The wheel-workpiece interaction modeling is based on three-dimensional geometric numerical model: calculating the penetration between the envelope contour of grinding wheel and workpiece.

The three-dimensional geometric contour of the grinding wheel and workpiece are usually digitized by stylus instrument or optical sensing,[38,39] and the macro geometric model of the grinding wheel can be obtained by combining contour elements.[40] Fig. 4 shows the kinematic equations of common grinding methods. Three traditional grinding methods (such as surface, cylindrical, inner cylindrical and plunge grinding) can get a general equation set by transforming and introducing

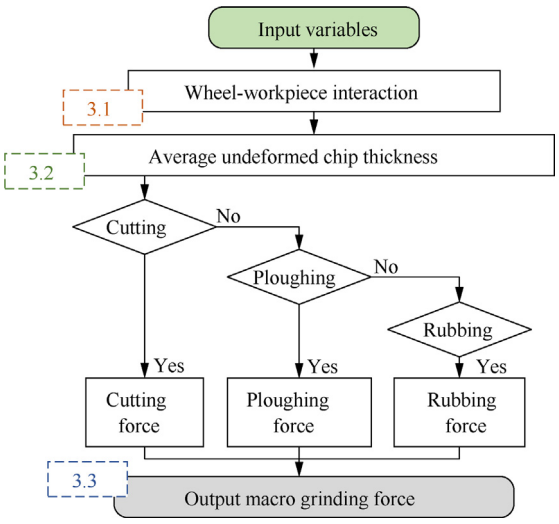

Fig. 3 Modeling method of macro grinding force.

kinematic parameters. The model is only suitable for simple coupling motion and is based on the plane rectangular coordinate system. But the more complicated grinding process needs special consideration, such as thread grinding, the inclination angle φ of grinding wheel is also considered, and the changed orthogonal coordinate system of grinding wheel is established.[41–43] The above grinding methods all set up the center to fix the workpiece. For centerless grinding, the circumference of the workpiece is fully supported by the grinding wheel, guide wheel and supporting blades[44].

3.2. Average undeformed chip thickness

The average undeformed chip thickness is defined as the distance between the active grain on the current grinding wheel track and the machined workpiece surface.[38] Several developed models to calculate average undeformed chip thickness are shown in Table 1. Pahlitzsch and Helmerdig[45] developed a simple model to determine the equivalent chip thickness. The model ignores the characteristic quantity and microstructure of grinding wheel morphology. In order to make the chip thickness model more realistic, it is assumed that the abrasive grains have uniform height, size and regular distribution, so the average undeformed chip thickness is the sum of the individual cutting thicknesses in the contact area between the grinding wheel and the workpiece, as shown in Eq.(1–2).[46] Similar to this model, Makin and Cook[47] introduced the ratio r of chip width to thickness, but the complexity of the actual chip shape[48] makes it difficult to get r. Furthermore, the influence of grinding wheel speed v_s and workpiece speed v_w on chip volume cannot be ignored.[49] With the in-depth understanding of the chip formation mechanism, the actual contact length l_c has been concerned as an important variable.[50,51] The contact length has three components, which are (a) the geometric grinding contact zone, (b) the elastic deflection between the wheel body and the workpiece and (c) the microscopic contact at the grain level. Werner's model[52] took the same form, but with different empirical coefficients, which depended on the specific geometry and trajectory of the grinding wheel.

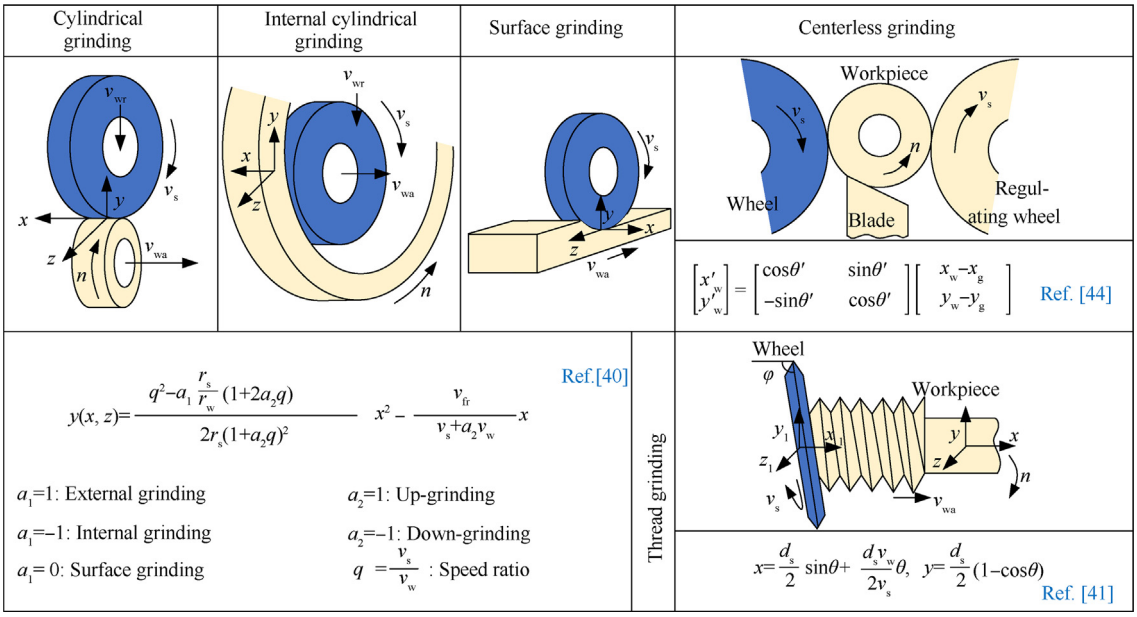

Fig. 4 Kinematics of common grinding methods.

Table 1 Several developed models to calculate average undeformed chip thickness.

Authors	Equations	Number
Pahlitzsc and Helmerdig[45]	$h = 2\lambda \frac{v_w}{v_s}\sqrt{\frac{a_p}{d_s}}$	(1-1)
Reichenbach, et al.[46]	$h = \left[\frac{4v_w}{v_s N c}\sqrt{a_p/d_s}\right]^{1/2}$	(1-2)
Makin and Cook[47]	$h = \left[\frac{4}{Cr}\left(\frac{v_w}{v_s}\right)\left(\frac{a_p}{d_{eq}}\right)^{\frac{1}{2}}\right]^{\frac{1}{2}}$	(1-3)
Agarwal, et al.[50,51]	$h = \sqrt{\frac{a_p v_w}{N v_s}\frac{1}{l_c}}$	(1-4)
Werner[52]	$h = \frac{1}{A}\left(\frac{2}{N}\right)^{1/\alpha+1}\left(\frac{v_w}{v_s}\right)^{1/\alpha+1}\left(\frac{a_p}{s_s}\right)^{1/2(\alpha+1)}$	(1-5)

Table 2 Macro grinding force models.

Authors	Models	Grinding stages
Salje[23]	$F_t = \tau_0 A$	Cutting
Werner and Konig[29]	$F_n = A\left(\frac{C^2}{K_1}\right)^{\frac{1-m}{3}}$	Cutting
Inasaki, et al.[53]	$F_n = \lambda b\left(\frac{v_w}{v_s}a_p\right)^{\varepsilon}$	Cutting
Li and Shin[54,55]	$F_n = K_r\frac{2\pi}{v_s N_r}(v_t\sin\theta + v_n\cos\theta)N_a$	Cutting
Chiu and Malkin[28]	$F_n = \frac{k_1 u_{ch} a v_w}{v_g} + k_2 F_{t,p} + p_c\sqrt{d_e a}Q$	Cutting, Ploughing Rubbing
Guo, et al.[56–58]	$F_n = K(v_w/v_s)a_p + K_1(v_w/v_s)d_e^{-0.5}a_p^{0.5} + K_4(v_w/v_s)^a d_g^b C_s d_e^{0.5}a_p^{0.5+c}$	Cutting, Ploughing Rubbing

3.3. Determination of macro grinding force

The macro grinding force can be calculated based on the average undeformed chip thickness. According to the grinding stages, some main research results of macro grinding force are shown in Table 2. The early macro grinding force model[23,29] mainly considered the experimental coefficient and the properties of materials. Inasaki, et al.'s model[53] consists of physical parts of speed ratio, grinding wheel width and grinding depth. Li and Shin[54,55] put forward the grinding force model of internal grinding, and introduced the number of active abrasive grains, which need a lot of experimental tests. Chiu and Malkin's model[28] considers three grinding stages, and innovatively considers the wear phenomenon caused by the friction between grinding wheel and workpiece. However, Chiu and Malkin's model does not consider the process change of the number of active abrasive grains. On this basis, Guo, et al.[56–58] put forward the grinding force model of cylindrical grinding, which is mainly used for the analysis of grinding dynamics. Although the grinding force model provides experience for the analysis of system dynamics, it does not consider the time-varying stiffness,[53] workpiece chatter regeneration effect[59] and chatter boundary.[54,55] It is the future development trend to make the dynamic characteristics of macro grinding force model more in line with actual machining.

3.4. Influence of unconventional grinding on macro grinding force model

In order to improve the force performance of traditional grinding, some non-traditional grinding methods, such as ultrasonic assisted grinding, robotic assisted grinding, electrochemical assisted grinding and laser assisted grinding, have been developed rapidly, and their machining characteristics have also

been considered in the establishment of macro grinding force model. According to the different influence mechanism of grinding force, the classification of grinding methods is shown in Fig. 5.[60-91]

The working principle of ultrasonic vibration is to control the ultrasonic power[92] and high-frequency vibration[64] by adjusting the ultrasonic generator, so as to change the movement track of abrasive grains. The specific equations of abrasive grain trajectory length are related to grinding conditions, such as side grinding,[77] end grinding,[27,93] surface grinding[92] and up grinding.[75] The grinding force under the action of ultrasonic wave is proved to be significantly lower than that of conventional grinding (CG),[94,95] and the stability of the grinding force of ultrasonic assisted grinding (UAG) is slightly better than that of CG. The mechanism of UAG on grinding force can be summarized as the periodic movement of abrasive grains changes the geometric shape and size of chips. Most of the chip shapes are flow patterns, especially at large amplitude.[96] The cross-sectional area and average length of chips corresponding to UAG are smaller than those of conventional grinding.[97,98] This is mainly because the ultrasonic vibration effectively reduces the friction coefficient between the abrasive grains and the chips, resulting in an increase in the shear angle of the chips, and ultimately a decrease in the thickness of the chips. The smaller chip length corresponding to UAG is mainly because the ultrasonic vibration promotes chip breakage. These phenomena are important factors affecting the grinding force of UAG.

The force instability caused by weak stiffness should be considered in the robotic assisted grinding force modeling.[78,79] Low stiffness and end-effector path tracking error are very sensitive to the magnitude and direction of grinding force.[99,100] Tahvilian, et al.[79] considered the stiffness of the grinding wheel and the impact times of each rotation of the grinding wheel, and calculated the average force by integrating the instantaneous force of one rotation of the grinding wheel. The robotic assisted grinding force model can be divided into impact stage, pressure relief stage and stable stage.[82] The grinding force in the impact stage changes rapidly in a short time, the increasing grinding depth in the pressure relief stage makes the grinding force unstable and the stabilization stage is related to the deformation caused by the low stiffness of the robot system. Although the grinding force is divided in detail, the force instability is still unresolved. Usually, the sudden change of grinding force can be reduced by feedback and path planning.[81] According to the global detection of grinding force signal, linear regression technology is applied to the calculation of grinding force coefficient.[101] However, optimization of grinding force requires many experimental results, and all possible subsets of parameters should be studied such as the deflection angle of the manipulator and the geometric size of the grinding wheel.

The consideration of laser and electrochemical assisted technologies in grinding force models is relatively late. Laser assisted methods is introduced because of its non-contact processing and high efficiency, including softening and structuring of workpiece materials. The soften effect induced by laser irradiation can decrease the normal indentation force and increase the scratching, ploughing and chips formation influence.[90] It is reported that different types of surface textures obtained by laser technology will also significantly affect the grinding force,[102] and the microstructure makes the interaction between abrasive grains and workpiece intermittent, thus reducing the total grinding force.[88,103] The principle of electrochemical

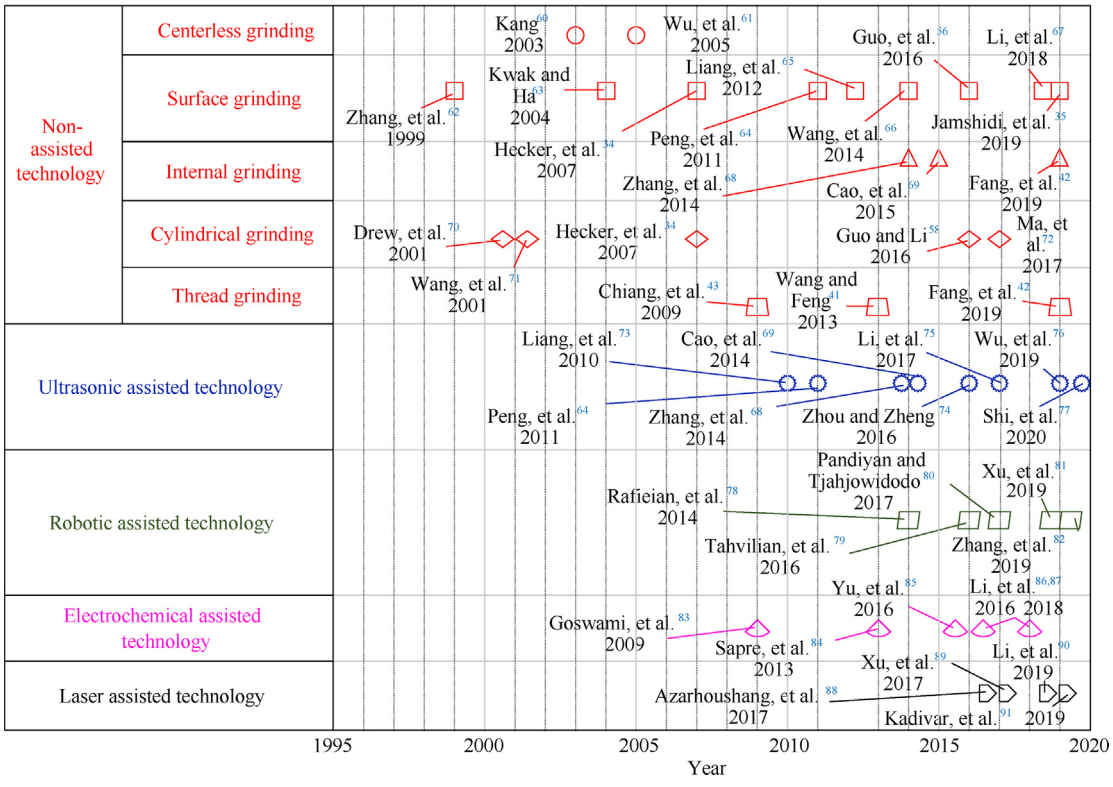

Fig. 5 Grinding force modeling under different grinding methods.

assisted technology is basically the same as that of laser softening: the electrolyte flow can change the material performance, which is beneficial to material removal, thus reducing grinding force.[84] The extremely low Vickers microhardness of the workpiece surface makes the grinding force lower than the untreated workpiece material.[87] Multi-field auxiliary processing technology has developed rapidly in recent years. However, there are few studies related to grinding force modeling. Future research on grinding force modeling will be reflected in the influence of laser temperature field or ultrasonic wave on workpiece material and chip properties.

4. Modeling process of micro grinding force

The modeling process of micro grinding force can be summarized as Fig. 6. The material properties is analyzed as the foundation (Section 4.1). Then the kinematics of abrasive grains under specific grinding conditions is calculated (Section 4.2), and the height distribution (Section 4.3) and number (Section 4.4) of abrasive grains are counted. Active abrasive grains with undeformed chip thickness greater than 0 are selected (Section 4.5), and the grinding force of single abrasive grain is analyzed (Section 4.6). Finally, the grinding forces of all active abrasive grains are accumulated to obtain the total grinding force (Section 4.7).

4.1. Foundation of micro grinding force modeling

The material properties of the workpiece affect the material removal mechanism, thus affecting the generation process of grinding force. The removal process of ductile materials includes rubbing force, ploughing force and cutting force,[104] as shown in Fig. 7. The cutting force is the largest,[105] followed by ploughing force and rubbing force.[37] The relationship among grinding depth, force components and deformation state should be considered in the process of modeling grinding force.[58,106] However, the existing models mainly focus on cutting force modeling, and do not consider the influence of workpiece deformation on the actual grinding depth, which will change critical value of grinding depth.

The grinding force model of brittle materials can be divided into three states: ductile, ductile–brittle transition and brittle, as shown in Fig. 8. Under low grinding force, abrasive grains plow out of grooves, and materials are taken away by plastic flow, resulting in plastic deformation of materials and ductile grinding grooves in the subsurface region.[107] With the increasing grinding force, central cracks and lateral cracks will be formed under abrasive grains. After brittle fracture, the grinding force begins to fluctuate obviously, and the fluctuation of thrust force is more serious than that of cutting force, which indicates that the surface damage is more serious.[108] Because the fracture mechanisms of brittle and ductile removal methods are different (crack propagation and grain breakage will replace the chip formation area), it is of great significance to study the critical state of ductile–brittle transition.

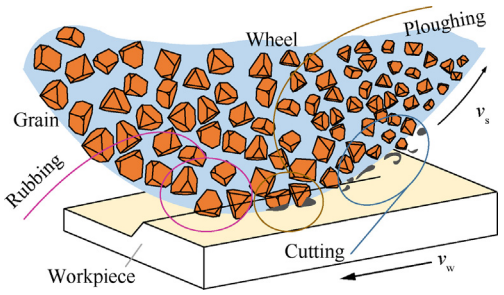

Fig. 7 Ductile material removal process considered in micro grinding force modeling process.

4.2. Active abrasive grain trajectory

The ways that affect the trajectory of abrasive grains include self-excited vibration and forced vibration.[90,109] Self-excited vibration depends on grinding parameters, grinding wheel type and grinding wheel life, and its vibration frequency is close to the natural frequency of mechanical system.[53] The self-excited chatter of grinding wheel will bring chatter marks, which should be avoided by setting grinding parameters and grinding wheel types in the actual grinding process.[110] Forced vibration depends on the eccentric force, unbalance force, stiffness and damping of the grinding wheel spindle.[111] This kind of vibration source can be located by frequency measurement and suppressed. Under different vibration conditions, the expression of abrasive trajectory is shown in Table 3. In forced vibration, the influences of eccentricity,[35,36] swing[112] and run-out[76] on abrasive grains need to be considered. In addition, actively applied UAG[74,92,113] is also a common means to change the trajectory of abrasive grains. Jamshidi, et al.'s model[35,36] considers the actual eccentric condition of grinding wheel and establishes the deterministic kinematics equation. However, the assumption that the distance between all adjacent grits along the periphery of the wheel surface is the same is obviously contrary to the real grinding wheel topography. In Zhou, et al.'s model,[112] the movement process of a single abrasive grain under different swing angles is established, but the

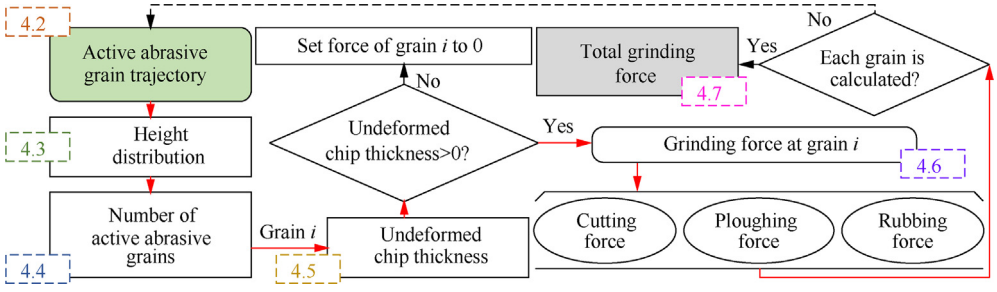

Fig. 6 General modeling process of micro grinding force.

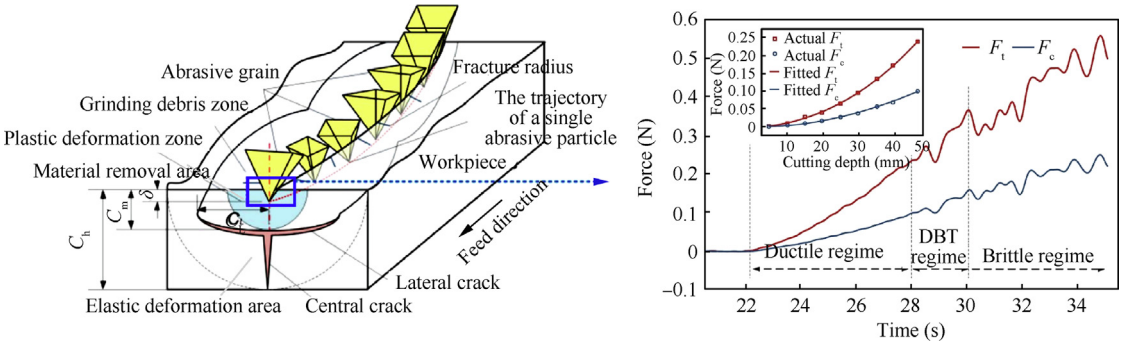

Fig. 8 Brittle material removal process considered in macro grinding force modeling process.[94] Copyright 2022 by Elsevier.

Table 3 Trajectory expressions of each abrasive grain.

Authors	Models	Dynamic factors
Jamshidi, et al.[35,36]	$\begin{cases} x_i = [R_i + R_0 \sin(\theta_i/2)]\sin(\theta_i) + ft \\ y_i = [R_i + R_0 \sin(\theta_i/2)](1 - \cos(\theta_i)) \end{cases}$	Deflection
Zhou, et al.[112]	$\begin{cases} x_i = r\sin(\omega t) \\ y_i = v_\omega t + r\cos(\omega t) \end{cases}$	Swing
Wu, et al.[76]	$\begin{cases} x_i = R\sin(\omega t - 2\pi m/M) + r\sin(\omega t + \alpha_0) \\ \quad + F_x(L - a_F)^2(2L + a_F - 3z)/(6EI) + f_v t \\ y_i = R\cos(\omega t - 2\pi m/M) + r\cos(\omega t + \alpha_0) \\ \quad + F_y(L - a_F)^2(2L + a_F - 3z)/(6EI) \end{cases}$	Run-out

impact of vibration caused by swing on the grinding force modeling was ignored. This problem is also reflected in the modeling process of grinding wheel vibration and run-out[76].

4.3. Determination of the height distribution of active abrasive grains

The protruding height of abrasive grains is defined as the height of the abrasive grain tip from the bonding surface/substrate.[112] The low height of abrasive grains and the small space for accommodating abrasive grains lead to the increase of grinding wheel load, which leads to the increase of grinding force.[114] The fresh grinding wheels after truing are generally considered that the distribution of the protruding height of abrasive grains follows the normal distribution law.[115,116] However, contradictory results have been found through profile measurement, there are both exponential distribution and normal distribution of abrasive protrusion height.[117] The result of this difference is that the abrasive grains are broken and shed in different degrees due to different truing conditions.[114] According to Vairamuthu, et al.,[118] normal distribution can well fit the surface shape of fresh wheels, but it cannot correctly represent damaged wheels, this is because active abrasive grains with high height will lose their peak value. Considering this phenomenon, extreme value distribution fitting method[35,119] can be used for this negative skewness phenomenon. For the height of abrasive grains before and after wear, if it does not conform to the normal distribution, specific mathematical methods can be adopted, such as Johnson transformation.[120] The data of normal distribution can be modified by modifying function. Abrasive wear will affect the height of abrasive grains and then change the component of grinding force, as shown in Fig. 9. In order to better represent the wear situation, the attack angle of the grain β, worn height distribution function $f(h)$, abrasive contact density ρ[121] and the wear rate I_V[106,122] are used to characterize the wear state. Although the dynamic process of changing the tip shape into a flat cone is considered, the random inclination angle of abrasive grains is not considered, which cannot ensure that abrasive grains participate in grinding in a cone shape.

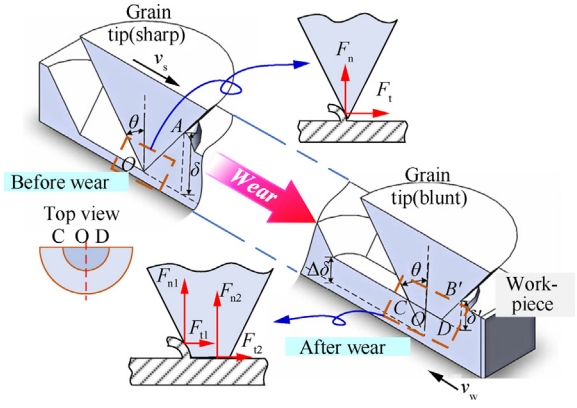

Fig. 9 Abrasive wear process considered in force modeling process.[122] Copyright 2022 by Elsevier.

4.4. Determination of the number of active abrasive grains

The number N of active abrasive grains is comprehensively influenced by static abrasive grain density and dynamic abrasive grain density, which can be expressed as[26,123]:

$$N = C_s b v_s t \tag{2}$$

where b is grinding width, t is grinding time. Grinding wheel surface can be copied by specific materials, but the operation is complicated and time-consuming and it is difficult to obtain satisfactory results.[124–126] A non-contact and non-destructive scanning system for directly measuring the surface of grinding wheel was proposed.[127] The principle is to scan the surface of grinding wheel with white light chromatic sensor and processed by image processing technology.[128] This method ensures the authenticity of scanned data and saves a lot of time. In addition to statistics, the removal amount of materials is applied to the modeling of abrasive density: $C_s(z) = C_s(z')(1 - V_{sh} / V_t)$.[129] This method verifies the dynamic change of the number of abrasive grains from the point of view of volume removal rate, but the number of abrasive grains calculated according to the removed volume is average, which can not characterize the process wear and breakage of abrasive grains. Cai and Rowe[127] used the abrasive grains at the top of the grinding wheel surface as a benchmark, and obtained the abrasive grain density by judging the relationship between the radial depth and the theoretical maximum undeformed chip thickness. However, the theoretical undeformed cutting thickness varies with different grinding wheels, and the active number of abrasive grains in the actual grinding process is not provided. Jamshidi, et al.[35] considered the self-excited vibration of grinding wheel, but the assumption of uniform distribution of abrasive grains was unreasonable. Based on the above static abrasive density model, a dynamic abrasive density model of engineering grinding wheel was proposed, and the influence of grinding wheel speed, workpiece speed and grinding depth on abrasive density was analyzed.[130] Common dynamic grinding parameters are considered, but the dynamic density of abrasive grains is composed of static density of abrasive grains and dynamic effects such as local deflection and dynamic hiding of abrasive grains, the dynamic effects of abrasive grains are still not paid attention to. Considering that there are many restrictions on dynamic abrasive grains, the dynamic density of abrasive grains is always lower than the static density,[69,33] which can be explained by Eq. (3)[129].

$$C_d(z) = \frac{C_s(z)}{1 + \frac{1}{3}\frac{C_s(z)}{z}\frac{\tan(\theta)}{\tan(\varepsilon)}E(h^3)} \tag{3}$$

where $C_s(z)$ is the static abrasive grain density, $C_s(z) = C_s(z')(1\text{-}V_{sh}/V_t)$. This model clearly shows the corresponding relationship between static abrasive density and dynamic abrasive density, but the equation is calibrated based on empirical force model. The empirical force model does not consider the dynamics of the process, which will affect the authenticity of the abrasive density. It is an important subject to establish a more comprehensive analysis model based on the density of active abrasive grains, and this influence should be included in the refinement of Eq.(7). At present, most models of abrasive grain number mainly focus on verification and statistics of static or uniform abrasive grain number, the process change of dynamic active abrasive grain number needs to be further clarified.

4.5. Calculation of instantaneous undeformed chip thickness

The model of instantaneous undeformed chip thickness needs to consider the influence of statistics and dynamics, which is an effective means to explain the instantaneous removal behavior of material. However, the improvement of model accuracy also means that the difficulty of modeling and data processing increases, which often takes a lot of time.

The difficulty of statistical model is mainly reflected in measurement and filtering. The undeformed chip thickness model based on grain height characteristics and active grain spacing can be expressed as Eq. (4-1)[131] in Table 4. The Kaliszer's model[131] is formulated under the condition that the wheels are stationary. On this basis, such as Eq. (4-2) and Eq. (4-3), the introduction of motion parameters such as dynamic height difference[36] and tangential angle position[120] in the actual grinding process is very critical. Statistical models provide better understanding of the grinding process,[132] Gaussian distribution [Eq. (4-4)[133]] and Rayleigh distribution [Eq. (4-5)[34]] are the probabilistic characterization models which are most commonly used. The former has centralization, symmetry and uniform variability, while the latter has the advantage of being uniquely defined by one parameter (σ). It has been proved that Rayleigh distribution in hard and brittle materials,[49,134] alloy materials,[34] metal materials,[42] etc. have high accuracy. However, most of the above probability models of chip thickness distribution are based on assumptions, and more work is needed to verify the unknown materials by experiments.

The above-mentioned instantaneous undeformed chip thickness is based on the ideal kinematics, however, some inevitable dynamic factors need to be considered in the grinding process: the regenerative vibration caused by the circumferential eccentricity,[135] runout,[35] deflection[76] and other errors of the grinding wheel profile. The instantaneous chip thickness of a single abrasive grain cross section is composed of three factors: (a) motional static undeformed chip thickness $h_{cu,0}$, (b) dynamic chip thickness $\Delta h_{cu,i}$ and (c) dynamic chip thickness deviation $\delta h_{cu,i}(\phi_i)$,[136] as shown in Eq.(5). More attention should be paid to the problem of multiple coupling between dynamic error and different active abrasive grains, and the

Table 4 Several developed models to calculate the undeformed chip thickness.

Authors	Models	Number
Kaliszer[131]	$h = 2s\left(\frac{a_{j-1}}{d_s}\right)^{1/2} - \delta_j$	(4-1)
Jamshidi and Budak[36]	$h = R_{n,j} - R_{m,j} + (n-m)f_t\sin(\theta_{i,j}) + n_{i,j}$	(4-2)
Ding, et al.[120]	$h = 2\lambda_j\frac{v_w}{v_s}\left(\frac{a_{j-1}}{d_s}\right)^{1/2} -2\frac{v_w}{v_s}\left(1+\frac{v_w}{v_s}\right)\left[a_{j-1} - \left(a_j a_{j-1}\right)^{1/2}\right]$	(4-3)
Wu, et al.[133]	$f(h) = \frac{1}{\sqrt{2\pi}\sigma_g}e^{\left[-\left(h-\bar{h}\right)^2/\left(2\sigma_g^2\right)\right]}$	(4-4)
Hecker, et al.[34]	$f(h) = \left(h/\sigma^2\right)e^{-h^2/2\sigma^2}$	(4-5)

undeformed chip thickness modeling technology of single abrasive grain should be applied to multiple abrasive grains on the whole surface of grinding wheel.

$$h = \pm h_{\mathrm{cu},0} + \Delta h_{\mathrm{cu},i} + \delta h_{\mathrm{cu},i}(\phi_i) \tag{5}$$

4.6. Determination of micro grinding force

Micro grinding force is influenced by structural parameters, motion parameters, material parameters, process parameters.[137] Part of micro grinding force models for removing ductile or brittle materials are listed in Table 5.[34–36,103,129,136,138]

For ductile materials, at first, Hecker, et al.'s model[34,129] has done a lot of work on the number of active abrasive grains. However, the structural parameters are still simplified, and the geometric shapes of abrasive grains are not counted and analyzed. The same problem is also reflected in Chen, et al.'s model[136] and Jamshidi, et al.'s model.[35,36] Although these models deeply discuss the influence of main excitation sources on dynamic grinding force, it is not desirable to simplify the distance between abrasive grains. Considering the above problems, Li, et al.'s model[139] considers the numerical analysis of the shape, size and position of abrasive grains, but the influence of dynamic effect on the time delay of grinding force is a problem to be clarified. Most of the macro grinding force models are for industrial metals. The grinding force of brittle materials is mainly affected by the interaction between single abrasive grains and the material, mainly for material fracture and breakage. At present, brittle materials use micro grinding force models, which is more conducive to focusing on micro behavior. Therefore, for brittle materials, the micro grinding force model is generally used instead of the macro grinding force model. For brittle materials, it has not been well studied as in ductile materials. It can also be seen from Wang, et al.'s model[138] and Zhang, et al.'s model[103] that there are still experimental coefficients in the force expression. This is because the current research work about hard and brittle materials mainly focuses on the process exploration of machining accuracy. With the improvement of understanding of material removal mechanism of brittle materials, micro grinding force modeling technology will also develop rapidly.

4.7. Superposition principle of micro grinding force

Vector superposition of grinding forces on all effective abrasive grains on the grinding wheel is a necessary way to transform micro grinding forces into total grinding forces, and an important means to verify and apply the grinding force model. In order to obtain the result of grinding force quickly and conveniently, the grinding force can be homogenized. The total grinding force on the whole grinding wheel can be expressed as the product of the number of grains in the grinding area and the micro grinding force of a single abrasive grain.[34,41,75,67] However, this method cannot accurately obtain the exact analytical solution of the total grinding force. So a more optimized model was proposed: combined time-domain model method and grinding mechanism, the dynamic grinding force was regarded as the sum of segmented forces along the contact length of the wheel in the whole processing time.[72] The grinding force on a certain contact length is accurately calculated by the segmented force model, which improves the accuracy of the model to a certain extent.

$$F = \int_{\theta_s - \Delta\theta}^{\theta_s} F(t_i) dl_c(t_i) \tag{6}$$

where $F(t_i)$ is function of segment force, θ_s is wheel degree. The grinding forces[136,36] in the grinding process are obtained by superimposing the force of each moving grain independently, and the equation is as follows:

$$\begin{bmatrix} F_x \\ F_z \end{bmatrix} = \sum_{i,j} \left(\begin{bmatrix} -\cos\theta_{i,j} & -\sin\theta_{i,j} \\ \sin\theta_{i,j} & -\cos\theta_{i,j} \end{bmatrix} \times \begin{bmatrix} Ft_{i,j} \\ Fn_{i,j} \end{bmatrix} \right) \tag{7}$$

where $\theta_{i,j}$ is rotational position angle of individual abrasive grain. However, when considering the material removal mechanism of abrasive grains, the grinding forces in the required grinding stage should be superimposed, so that the total grinding forces are closer to the actual machining situation. From the development of superposition model, it can be seen that the improvement of superposition principle will lead to a fine micro grinding force model. Therefore, it is an important research content to deeply understand the influence of superposition principle on grinding force results, which should be included in the refinement of Eq.(6).

Table 5 Micro grinding force models.

Authors	Models	Grinding stage
Hecker, et al.[34,129]	$F_n = d_f \frac{HB\pi D}{2}\left(D - \left(D^2 - d^2\right)^{1/2}\right) \cdot(\cos\alpha - f\sin\alpha)$	Cutting
Chen, et al.[136]	$F_n = c_s K_s [v_w/v_s]^{2\varepsilon-1} [d_s]^{1-\varepsilon} h_{cu,i}(\phi_i) d\phi$	Cutting
Jamshidi, et al.[35,36]	$F_n = K_{nc} w_c h_{i,j}(\theta_{i,j}) + K_{ne} w_c$	Cutting, Ploughing
Wang, et al.[138]	$F = \frac{1}{3} E (8d)^{\frac{1}{2}} \delta_b^{\frac{3}{2}} / (1 - \nu^2)$	Ductile Brittle
Zhang, et al.[103]	$F = \left(\frac{d_{gc}^2 (15 l_d + 16 l_c) \cot^{\frac{1}{4}}\theta H^{\frac{3}{2}} K_{IC}^{\frac{1}{2}} \left(1-\nu^2\right)^{\frac{1}{4}}}{192 E^{\frac{7}{8}} \eta^2 l_c} \right)^{\frac{8}{9}}$	Ductile-to-brittle transition

5. Applications of grinding force model

The grinding force model can accurately predict the grinding results, optimize the grinding conditions and control the grinding process. In the following, the beneficial application of grinding force model in chatter suppression, force control technology and other grinding process simulation will be reviewed.

5.1. Chatter suppression

It is demonstrated that the instability of dynamic grinding force might be traced back to frictional chatter,[140] mode coupling,[141] thermo-mechanical instability,[142] and other complex effects due to system non-linearities.[143] Due to the unstable grinding force, it usually leads to production loss and high rejection rate of products,[144] so it is necessary to analyze and suppress the chatter properties from the perspective of grinding force. Although the grinding force is applied to the above vibration models, the expressions of the grinding force still have obvious average characteristics, and the composition of dynamic components is not considered. Based on this problem, the grinding force is established from the perspective of

dynamic frequency domain,[58] and applied to the nonlinear analysis of machine tool system. Even so, we should realize that although the theoretical modeling of grinding force has gained rapid attention and development in recent years, the expression of $F(t)$ in the Eq.(8) has not been updated in the dynamics of machine tools[145].

$$\begin{cases} F_x(t) = m_x\ddot{x}(t) + c_x\dot{x}(t) + k_x x(t) \\ F_y(t) = m_y\ddot{y}(t) + c_y\dot{y}(t) + k_y y(t) \end{cases} \tag{8}$$

where m, c and k are modal mass, damping and stiffness values in the feed or normal directions. As shown in Fig. 10,[93,136,146] it can be clearly observed from the naked eye that the unstable grinding force will bring a lot of ripples to the surface. As the grinding force model becomes more and more complex and accurate, it will provide strategies to solve the chatter problem from the perspective of the nonlinear system of machine tool-tool rest-tool-workpiece.

5.2. Force-control technique

The deflection and material removal rate of the machine tool can be adjusted accurately by combining the grinding process model with the force control during the grinding process, which can improve the repeatability of the shape and finishing of the resulting parts.[147,148] Hahn and Robert[149] first proposed the idea of controlled-force grinding, but the idea is only suitable for short-stroke grinding operation. For the conventional grinding process, the wear phenomenon of grinding wheel will also change the grinding force signal constantly. In order to reduce the workload of selecting grinding parameters and maintain the stability of grinding process, many force-control grinding strategies have been proposed, such as feedback control system[150] and adaptive control system.[151] The two control systems generally belong to the fully closed-loop control technology, and the processing parameters (feed speed, feed amount, etc.) are adjusted in real time through online detection of machine tool processing variables (mainly grinding force). Therefore, the grinding force model determines the feasibility of force control technology to a large extent, and is an indispensable part of optimizing the machining process of machine tools.

The grinding force controller is usually established according to the relationship between the difference between the grinding detection force (F_m) and the average cumulative force (F_c) and the predetermined benchmark (F_s), as shown in the following equation. The current force feedback control technology is mainly reflected in the force boundary control. For some ultra-precision grinding,[152,153] it may be a breakthrough technology to monitor and adjust all the force signal[154].

$$F_m - \frac{\Sigma F_c}{A_t} \geqslant F_s \tag{9}$$

Although the feedback control strategy can control the grinding force by adjusting the feed rate, the dynamic response of the controller is often required during the grinding process. Since the force-adaptive grinding strategy can make a strong response to any changes in the control variables, and can achieve the necessary process optimization.[155] Nonlinear adaptive control law has the characteristics of fast dynamic response, small overshoot, and high steady-state accuracy.[156] However, its relationship with force signals needs further explanation. The difference between the average current and the predetermined current is also used as an effective parameter for the induction grinding force feedback.[157]

The grinding force can be effectively reduced by the above grinding force control method, the stability of grinding process is controlled and the surface finish of workpiece is improved. However, some important parameters need to be considered in future research, such as capacitance shunt of piezoelectric ports.

5.3. Grinding process simulation

As an important parameter to evaluate the grinding performance, grinding force is also widely used in the grinding simulation. The grinding force directly affects the mechanical energy generated in the grinding process, and most of the mechanical energy is converted into heat.[158] Grinding force and heat can lead to huge defects such as surface microcracks, severe plastic deformation and surface burns.[159] Hyung and Steven[160] established a thermo-mechanical model of the grinding process based on micro grinding forces. Although the

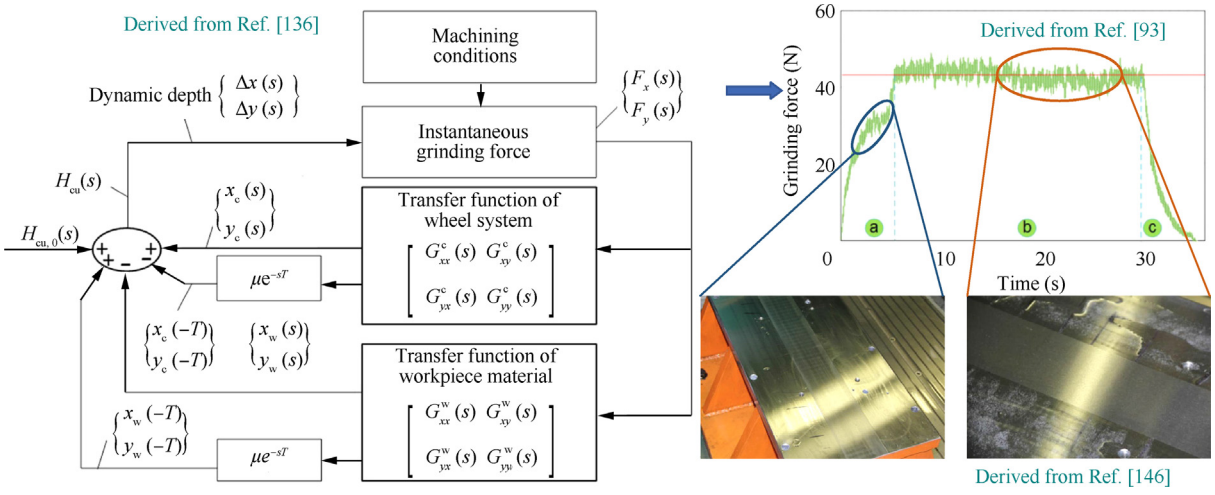

Fig. 10 Close-loop control system of grinding force. Copyright 2022 by Springer Nature and Elsevier.

ploughing and rubbing effects of force are considered when estimating the thermal effect, this is limited to a single abrasive grain and cannot reflect the real grinding process. Naskar, et al.[161] evaluated the effect of grinding force and heat on the integrity of abrasive grains. Due to the thermal shock, the abrasive grains usually undergo macro fracture, which plays a dominant role in the radial wear of the abrasive grains and the surface defects of the workpiece. The heat flux density curve of the whole grinding contact length can be established by grinding force[162].

$$q_{\mathrm{l}} = \frac{F_{\mathrm{t}} v_{\mathrm{s}}}{b\Delta l} R_{\mathrm{w}} \tag{10}$$

where R_{w} is the heat partition ratio to the workpiece. Yao, et al.[163] determined the maximum grinding temperature for the white alumina wheel and single alumina wheel. It can be judged that the grinding temperature is affected by the thermal conductivity γ of the grinding wheel and the tangential grinding force F_{t}.

$$T_{\max} = \frac{\left(F_{\mathrm{t}}' v_{\mathrm{s}}^{1.5} - 5.16 \times 10^{9} a_{\mathrm{p}} v_{\mathrm{w}} \sqrt{v_{\mathrm{s}}}\right)}{172.24 \sqrt{v_{\mathrm{w}} \sqrt{a_{\mathrm{p}}}} \left(47.52 \sqrt{v_{\mathrm{s}}} + \gamma\right) + 3600 \sqrt{v_{\mathrm{s}} a_{\mathrm{p}}}} \tag{11}$$

However, this model is based on the experimental coefficient, which is special. Based on this model, Liu, et al.[159] established a general expression of the highest grinding temperature quantitatively expressed by grinding force.

$$T_{\max} = \lambda R_{\mathrm{w}} \frac{F_{\mathrm{t}} v_{\mathrm{c}}}{\beta_{\mathrm{w}} S} \sqrt{\frac{l_{\mathrm{c}}}{v_{\mathrm{w}}}} \tag{12}$$

where λ is temperature constant for workpiece conduction, β_{w} is the thermal contact coefficient, q_{w} is heat flux into the workpiece part. However, it should be noted that F_{t} does not reflect the dynamic action of grinding force. It is an important subject to deeply understand the influence of abrasive grain characteristics on micro-scale heat transfer performance[164,165].

Grinding force model is also the key to solve the theoretical problems of contact deformation, stress field distribution and subsurface defects. The local contact deformation required by force balance can be solved by iterative method[44] and laplace transfer function,[154] thus realizing the control of grinding force on contact deformation. For the stress field distribution, the residual stress distribution over the whole grinding length can be obtained by using the grinding force in the finite element model.[162] The ripple attenuation rate of abrasive grains can be predicted by the frequency characteristics of grinding force.[61] And the wear condition of the grinding wheel can be monitored by measuring the grinding force, so that the grinding wheel can be repaired or replaced in time.[14] As a kind of random signal, grinding force signal has rich connotation and can reflect the performance of grinding process in real time. How to make good use of the information brought by the grinding force signal, so as to better formulate the grinding process and reduce the grinding cost, this is a problem that needs to be seriously considered.

6. Conclusions

Most of the grinding force models have been proposed and developed in the past 20–25 years, but they are often based on older and simple modes. The grinding force modeling can be divided into micro and macro grinding force modeling according to whether the influence of abrasive grains is considered. The key technologies involved in grinding force model are summarized, such as chatter suppression, force-control technology and grinding process simulation. To sum up, we can get conclusions:

(1) In the past 15 years, grinding force modeling technology has been greatly developed. More and more studies have proved that grinding force modeling is promising. Grinding force modeling can quantitatively describe the dynamic process of relative vibration, which helps to evaluate the dynamic interaction in grinding process.

(2) The macro grinding force model takes the grinding wheel as a whole and is based on average parameters and force coefficients in grinding process. Macro grinding force model is mostly used for production practice and phenomenon description, and has the characteristics of high efficiency. However, a lot of calibration experiments are needed for different processing conditions to improve the accuracy of fitting coefficient.

(3) Micro grinding force modeling is based on the interaction between active abrasive grains and workpiece, focusing on the randomness and difference caused by abrasive grains, considering grinding geometry and grinding kinematics. Micro grinding force model is an effective means to explain the transient change of grinding process. However, the improvement of model accuracy also means that a large amount of data and situations need to be considered, which often takes a lot of time.

(4) As an important parameter for evaluating the grinding process, grinding force models have been widely developed and applied in the field of chatter suppression, force-control technology and grinding process simulation. How to make good use of the information brought by the grinding force signal, so as to better formulate the grinding process and reduce the grinding cost, this is a problem that needs to be seriously considered.

7. Future works

This paper provides a critical review of the relevant literature on grinding force modeling and points out the current problems in grinding force research. In view of these problems, it can be expected that grinding force modeling will require further research in the following directions in the future.

(1) All the grinding force models put forward so far have simplified the reality to varying degrees. In the future, in order to obtain more accurate predictions, more processing factors need to be considered, such as thermal properties, lubrication conditions, etc., and the study of multi-factor coupled models is of great significance.

(2) For difficult-to-machine materials, such as carbon fibers, crystalline materials, and heterogeneous materials (multiphase materials, composite materials), it is necessary to consider the changing mechanism of material properties on grinding force.

(3) For non-traditional grinding, changes in the grinding environment need to be considered. The grinding wheel itself (eg additive manufacturing, structured grinding), extreme machining conditions and multi-field assisted machining require attention.

(4) The grinding force model has been widely used in engineering for monitoring and real-time feedback, which puts forward more stringent requirements for the solution method of grinding force. More advanced grinding force models need to be developed to meet the real-time application requirements.

Declaration of Competing Interest

The authors declare that they have no known competing financial interests or personal relationships that could have appeared to influence the work reported in this paper.

Acknowledgements

This study was co-supported by the Enterprise Innovation and Development Joint Program of the National Natural Science Foundation of China (No. U20B2032), National Natural Science Foundation of China (No. 51875135).

References

1. Doman DA, Warkentin A, Bauer R. Finite element modeling approaches in grinding. *Int J Mach Tools Manuf* 2009;**49**:109–16.
2. Guo CS, Shi ZD, Mullany B, et al. Recent advancements in machining with abrasives. *J Manuf Sci Eng Trans Asme* 2020;**142** 110810.
3. Guo J, Bai JM, Liu K, et al. Surface quality improvement of selective laser sintered polyamide 12 by precision grinding and magnetic field-assisted finishing. *Mater Des* 2018;**138**:39–45.
4. Zhu DH, Feng XZ, Xu XH, et al. Robotic grinding of complex components: a step towards efficient and intelligent machining - challenges, solutions, and applications. *Robotics Comput Integr Manuf* 2020;**65** 101908.
5. Guo B, Meng QY, Li S, et al. Pulse laser precision truing of the V-shaped coarse-grained electroplating CBN grinding wheel. *Mater Des* 2022;**217** 110650.
6. Li CH, Wang S, Zhang Q, et al. Evaluation of minimum quantity lubrication grinding with nano-particles and recent related patents. *Recent Pat Nanotechnol* 2013;**7**:167–81.
7. Li HN, Axinte D. Textured grinding wheels: a review. *Int J Mach Tools Manuf* 2016;**109**:8–35.
8. Guo B, Meng QY, Wu GC, et al. Parallel axis precision grinding of micro-tooth internal thread with the coarse-grains CBN wheels. *J Manuf Process* 2022;**74**:474–85.
9. Azarhoushang B, Zahedi A. Laser conditioning and structuring of grinding tools - a review. *Adv Manuf* 2017;**5**:35–49.
10. Yang M, Li CH, Zhang YB, et al. Maximum undeformed equivalent chip thickness for ductile-brittle transition of zirconia ceramics under different lubrication conditions. *Int J Mach Tools Manuf* 2017;**122**:55–65.
11. Duan ZJ, Li CH, Ding WF, et al. Milling force model for aviation aluminum alloy: academic insight and perspective analysis. *Chin J Mech Eng* 2021;**34**:18.
12. Deng H, Xu Z. Dressing methods of superabrasive grinding wheels: a review. *J Manuf Process* 2019;**45**:46–69.
13. Ding WF, Linke B, Zhu YJ, et al. Review on monolayer CBN superabrasive wheels for grinding metallic materials. *Chin J Aeronaut* 2017;**30**(1):109–34.
14. Huang H, Li XL, Mu DK, et al. Science and art of ductile grinding of brittle solids. *Int J Mach Tools Manuf* 2021;**161** 103675.
15. Brehl DE, Dow TA. Review of vibration-assisted machining. *Precis Eng* 2008;**32**:153–72.
16. Yang ZC, Zhu LD, Zhang GX, et al. Review of ultrasonic vibration-assisted machining in advanced materials. *Int J Mach Tools Manuf* 2020;**156** 103594.
17. Zhang YB, Li CH, Jia DZ, et al. Experimental evaluation of the lubrication performance of MoS_2/CNT nanofluid for minimal quantity lubrication in Ni-based alloy grinding. *Int J Mach Tools Manuf* 2015;**99**:19–33.
18. Zhang YB, Li CH, Ji HJ, et al. Analysis of grinding mechanics and improved predictive force model based on material-removal and plastic-stacking mechanisms. *Int J Mach Tools Manuf* 2017;**122**:81–97.
19. Zhang YB, Li HN, Li CH, et al. Erratum to: Nano-enhanced biolubricant in sustainable manufacturing: from processability to mechanisms. *Friction* 2022;1–2.
20. Cao HR, Zhang XW, Chen XF. The concept and progress of intelligent spindles: a review. *Int J Mach Tools Manuf* 2017;**112**:21–52.
21. Li Y, Zhao WH, Lan SH, et al. A review on spindle thermal error compensation in machine tools. *Int J Mach Tools Manuf* 2015;**95**:20–38.
22. Zhang SJ, To S, Zhang GQ, et al. A review of machine-tool vibration and its influence upon surface generation in ultra-precision machining. *Int J Mach Tools Manuf* 2015;**91**:34–42.
23. Saljé E. *Gesetzmäßigkeiten und kennzahlen beim schleifen*. RWTH Aachen University; 1952.
24. Brinksmeier E, Aurich JC, Govekar E, et al. Advances in modeling and simulation of grinding processes. *CIRP Ann* 2006;**55**:667–96.
25. Younis M, Alawi H. Probabilistic analysis of the surface grinding process. *Trans Can Soc Mech Eng* 1984;**8**:208–13.
26. Zhang N, Kirpitchenko I, Liu DK. Dynamic model of the grinding process. *J Sound Vib* 2005;**280**:425–32.
27. Zhang JH, Zhao Y, Tian FQ, et al. Kinematics and experimental study on ultrasonic vibration-assisted micro end grinding of silica glass. *Int J Adv Manuf Technol* 2015;**78**:1893–904.
28. Chiu N, Malkin S. Computer simulation for cylindrical plunge grinding. *CIRP Ann* 1993;**42**:383–7.
29. Werner G, Konig W. Influence of work material on grinding forces. *CIRP Ann* 1978;**27**:243–8.
30. Aslan D, Budak E. Surface roughness and thermo-mechanical force modeling for grinding operations with regular and circumferentially grooved wheels. *J Mater Process Technol* 2015;**223**:75–90.
31. Ozlu E, Molinari A, Budak E. Two-zone analytical contact model applied to orthogonal cutting. *Mach Sci Technol* 2010;**14** (3):323–43.
32. Law SS, Wu SM. Simulation study of the grinding process. *ASME Pap* 1972(72–WA/Prod–25): 972–8
33. Konig W, Lortz W. Properties of cutting edges related to chip formation in grinding. *CIRP Ann* 1975;**24**:231–5.
34. Hecker RL, Liang SY, Wu XJ, et al. Grinding force and power modeling based on chip thickness analysis. *Int J Adv Manuf Technol* 2007;**33**:449–59.
35. Jamshidi H, Gurtan M, Budak E. Identification of active number of grits and its effects on mechanics and dynamics of abrasive processes. *J Mater Process Technol* 2019;**273** 116239.
36. Jamshidi H, Budak E. An analytical grinding force model based on individual grit interaction. *J Mater Process Technol* 2020;**283** 116700.
37. Linke B, Garretson IC, Torner FM, et al. Grinding energy modeling based on friction, plowing and shearing. *J Manuf Sci Eng Trans Asme* 2017;**139** 121009.
38. Tönshoff HK, Peters J, Inasaki I, et al. Modelling and simulation of grinding processes. *CIRP Ann* 1992;**41**:677–88.
39. Inasaki I. Grinding process simulation based on the wheel topography measurement. *CIRP Ann* 1996;**45**:347–50.

40. Warnecke G, Zitt U. Kinematic simulation for analyzing and predicting high-performance grinding processes. *CIRP Ann* 1998;**47**:265–70.
41. Wang W, Feng XY. Analysis of grinding force and elastic deformation in thread grinding process. *Adv Mech Eng* 2013;**5** 827831.
42. Fang C, Yang CB, Cai LG, et al. Predictive modeling of grinding force in the inner thread grinding considering the effect of grains overlapping. *Int J Adv Manuf Technol* 2019;**104**:943–56.
43. Chiang CJ, Fong ZH, Tseng JT. Computerized simulation of thread form grinding process. *Mech Mach Theory* 2009;**44**:685–96.
44. Li HQ, Shin Y. A time domain dynamic simulation model for stability prediction of infeed centerless grinding processes. *J Manuf Sci Eng Trans Asme* 2007;**129**:539–50.
45. Pahlitzsch G, Helmerdig H. Determination and significance of chip thickness in grinding. *Workshop Technol* 1943;397–401.
46. Reichenbach GS, Mayer J, Kalpakcioglu S, et al. The role of chip thickness in grinding. *Trans ASME* 1956;847–50.
47. Malkin S, Cook NH. The wear of grinding wheels: part 1 – attritious wear. *J Eng Ind* 1971;**93**:1120–8.
48. Tso PL. An investigation of chip types in grinding. *J Mater Process Technol* 1995;**53**:521–32.
49. Tso PL, Wu SH. Analysis of grinding quantities through chip sizes. *J Mater Process Technol* 1999;**95**:1–7.
50. Agarwal S, Venkateswara RP. Predictive modeling of force and power based on a new analytical undeformed chip thickness model in ceramic grinding. *Int J Mach Tools Manuf* 2013;**65**:68–78.
51. Agarwal S, Venkateswara RP. Predictive modeling of undeformed chip thickness in ceramic grinding. *Int J Mach Tools Manuf* 2012;**56**:59–68.
52. Werner G. Kinematic and mechanic during grinding processes. *RWTH Aachen Univ* 1971.
53. Inasaki I, Karpuschewski B, Lee HS. Grinding chatter - origin and suppression. *CIRP Ann* 2001;**50**:515–34.
54. Li HQ, Shin Y. A time-domain dynamic model for chatter prediction of cylindrical plunge grinding processes. *J Manuf Sci Eng Trans Asme* 2006;**128**:404–15.
55. Li HQ, Shin YC. A study on chatter boundaries of cylindrical plunge grinding with process condition-dependent dynamics. *Int J Mach Tools Manuf* 2007;**47**:1563–72.
56. Guo MX, Li BZ, Ding ZS, et al. Empirical modeling of dynamic grinding force based on process analysis. *Int J Adv Manuf Technol* 2016;**86**:3395–405.
57. Guo MX, Jiang XH, Ding ZS, et al. A frequency domain dynamic response approach to optimize the dynamic performance of grinding machine spindles. *Int J Adv Manuf Technol* 2018;**98**:2737–45.
58. Guo MX, Li BZ. A frequency-domain grinding force model-based approach to evaluate the dynamic performance of high-speed grinding machine tools. *Mach Sci Technol* 2016;**20**:115–31.
59. Zhu XJ, Wang JQ, Cheng Q, et al. Research on dynamic grinding force in ultrasonic honing chatter. *Key Eng Mater* 2011;**487**:433–7.
60. Kang K. Modeling of the centerless through-feed grinding process. *KSME Int J* 2003;**17**:1036–43.
61. Wu YB, Wang J, Fan YF, et al. Determination of waviness decrease rate by measuring the frequency characteristics of the grinding force in centerless grinding. *J Mater Process Technol* 2005;**170**:563–9.
62. Zhang B, Wang JX, Yang FL, et al. The effect of machine stiffness on grinding of silicon nitride. *Int J Mach Tools Manuf* 1999;**39**:1263–83.
63. Kwak JS, Ha MK. Detection of dressing time using the grinding force signal based on the discrete wavelet decomposition. *Int J Adv Manuf Technol* 2004;**23**:87–92.
64. Peng Y, Wu YB, Liang ZQ, et al. An experimental study of ultrasonic vibration-assisted grinding of polysilicon using two-dimensional vertical workpiece vibration. *Int J Adv Manuf Technol* 2011;**54**:941–7.
65. Liang ZQ, Wang XB, Wu YB, et al. An investigation on wear mechanism of resin-bonded diamond wheel in Elliptical Ultrasonic Assisted Grinding (EUAG) of monocrystal sapphire. *J Mater Process Technol* 2012;**212**:868–76.
66. Wang DX, Ge PQ, Bi WB, et al. Grain trajectory and grain workpiece contact analyses for modeling of grinding force and energy partition. *Int J Adv Manuf Technol* 2014;**70**:2111–23.
67. Li J, Wang XL, Shen NY, et al. Modeling of acoustic emission based on the experimental and theoretical methods and its application in face grinding. *Int J Adv Manuf Technol* 2018;**98**:2335–46.
68. Zhao B, Li YM, Bian PY. Study of grinding force for internal cylinder of ultrasonic ELID composite grinding. *16th International Symposium on Advances in Abrasive Technology*; 2013 Sep 23-6; Hangzhou, China. 2014
69. Cao JG, Wu YB, Li JY, et al. A grinding force model for ultrasonic assisted internal grinding (UAIG) of SiC ceramics. *Int J Adv Manuf Technol* 2015;**81**:875–85.
70. Drew SJ, Mannan MA, Ong KL, et al. The measurement of forces in grinding in the presence of vibration. *Int J Mach Tools Manuf* 2001;**41**:509–20.
71. Wang WP, Peng YH, Li XY. Fuzzy estimation of uncertainty for grinding force. *11th Grinding and Machining Conference*; 2001 Jun 2-6; Quanzhou, China: Key Engineering Materials:2001.
72. Ma YC, Yang JG, Li BZ, et al. An analytical model of grinding force based on time-varying dynamic behavior. *Int J Adv Manuf Technol* 2017;**89**:2883–91.
73. Liang ZQ, Wu YB, Wang XB, et al. A new two-dimensional ultrasonic assisted grinding (2D-UAG) method and its fundamental performance in monocrystal silicon machining. *Int J Mach Tools Manuf* 2010;**50**:728–36.
74. Zhou M, Zheng W. A model for grinding forces prediction in ultrasonic vibration assisted grinding of SiCp/Al composites. *Int J Adv Manuf Technol* 2016;**87**:3211–24.
75. Li C, Zhang FH, Meng BB, et al. Material removal mechanism and grinding force modelling of ultrasonic vibration assisted grinding for SiC ceramics. *Ceram Int* 2017;**43**:2981–93.
76. Wu J, Cheng J, Gong YD. A study on material removal mechanism of ultramicro-grinding (UMG) considering tool parallel Run-out and deflection. *Int J Adv Manuf Technol* 2019;**103**:631–53.
77. Shi HY, Yuan SM, Zhang C, et al. A cutting force prediction model for rotary ultrasonic side grinding of CFRP composites considering coexistence of brittleness and ductility. *Int J Adv Manuf Technol* 2020;**106**:2403–14.
78. Rafieian F, Hazel B, Liu ZH. Vibro-impact dynamics of material removal in a robotic grinding process. *Int J Adv Manuf Technol* 2014;**73**:949–72.
79. Tahvilian AM, Hazel B, Rafieian F, et al. Force model for impact cutting grinding with a flexible robotic tool holder. *Int J Adv Manuf Technol* 2016;**85**:133–47.
80. Pandiyan V, Tjahjowidodo T. In-process endpoint detection of weld seam removal in robotic abrasive belt grinding process. *Int J Adv Manuf Technol* 2017;**93**:1699–714.
81. Xu XH, Zhu DH, Zhang HY, et al. Application of novel force control strategies to enhance robotic abrasive belt grinding quality of aero-engine blades. *Chin J Aeronaut* 2019;**32** (10):2368–82.
82. Zhang T, Xiao M, Zou YB, et al. Robotic constant-force grinding control with a press-and-release model and model-based reinforcement learning. *Int J Adv Manuf Technol* 2019;**106**:589–602.

83. Goswami RN, Mitra S, Sarkar S. Experimental investigation on electrochemical grinding (ECG) of alumina-aluminum interpenetrating phase composite. *Int J Adv Manuf Technol* 2009;**40**:729–41.
84. Sapre P, Mall A, Joshi SS. Analysis of electrolytic flow effects in micro-electrochemical grinding. *J Manuf Sci Eng Trans Asme* 2013;**135** 011012.
85. Yu XL, Huang ST, Xu LF. ELID grinding characteristics of SiCp/Al composites. *Int J Adv Manuf Technol* 2016;**86**:1165–71.
86. Li SS, Wu YB, Nomura M. Fundamental investigation of ultrasonic assisted pulsed electrochemical grinding of Ti-6Al-4V. *Mater Sci Forum* 2016;**4389**:279–84.
87. Li SS, Wu YB, Nomura M, et al. Fundamental machining characteristics of ultrasonic-assisted electrochemical grinding of Ti–6Al–4V. *J Manuf Sci Eng Trans Asme* 2018;**140** 071009.
88. Azarhoushang B, Soltani B, Zahedi A. Laser-assisted grinding of silicon nitride by picosecond laser. *Int J Adv Manuf Technol* 2017;**93**:2517–29.
89. Xu S, Yao ZQ, Cai HY, et al. An experimental investigation of grinding force and energy in laser thermal shock-assisted grinding of zirconia ceramics. *Int J Adv Manuf Technol* 2017;**91**:3299–306.
90. Li ZP, Zhang FH, Luo XC, et al. Material removal mechanism of laser-assisted grinding of RB-SiC ceramics and process optimization. *J Eur Ceram Soc* 2019;**39**:705–17.
91. Kadivar M, Shamray S, Soltani B, et al. Laser-assisted micro-grinding of Si_3N_4. *Precis Eng* 2019;**60**:394–404.
92. Li DG, Tang JY, Chen HF, et al. Study on grinding force model in ultrasonic vibration-assisted grinding of alloy structural steel. *Int J Adv Manuf Technol* 2019;**101**:1467–79.
93. Wang H, Hu YB, Cong WL, et al. A mechanistic model on feeding-directional cutting force in surface grinding of CFRP composites using rotary ultrasonic machining with horizontal ultrasonic vibration. *Int J Mech Sci* 2019;**155**:450–60.
94. Yang ZC, Zhu LD, Lin B, et al. The grinding force modeling and experimental study of ZrO_2 ceramic materials in ultrasonic vibration assisted grinding. *Ceram Int* 2019;**45**:8873–89.
95. Shen JY, Wang JQ, Jiang B, et al. Study on wear of diamond wheel in ultrasonic vibration-assisted grinding ceramic. *Wear* 2015;**332–333**:788–93.
96. Li SS, Wu YB, Nomura M. Effect of grinding wheel ultrasonic vibration on chip formation in surface grinding of Inconel 718. *Int J Adv Manuf Technol* 2016;**86**:1113–25.
97. Azarhoushang B, Tawakoli T. Development of a novel ultrasonic unit for grinding of ceramic matrix composites. *Int J Adv Manuf Technol* 2011;**57**:945.
98. Li H, Lin B, Wan SM, et al. An experimental investigation on ultrasonic vibration-assisted grinding of SiO_2f/SiO_2 composites. *Mater Manuf Process* 2016;**31**:887–95.
99. Díaz-Tena E, Ugalde U, de Lacalle LNL, et al. Propagation of assembly errors in multitasking machines by the homogenous matrix method. *Int J Adv Manuf Technol* 2013;**68**:149–64.
100. Liu L, Ulrich BJ, Elbestawi MA. Robotic grinding force regulation: design, implementation and benefits. *Proc IEEE Int Conf Robotics Autom* 1990;**1**:258–65.
101. Latifinavid M, Konukseven EI. Hybrid model based on energy and experimental methods for parallel hexapod-robotic light abrasive grinding operations. *Int J Adv Manuf Technol* 2017;**93**:3873–87.
102. Stępień P. Grinding forces in regular surface texture generation. *Int J Mach Tools Manuf* 2007;**47**:2098–110.
103. Zhang XH, Kang ZX, Li S, et al. Grinding force modelling for ductile-brittle transition in laser macro-micro-structured grinding of zirconia ceramics. *Ceram Int* 2019;**45**:18487–500.
104. Duan JH, Zhang YM, Shi YY. Belt grinding process with force control system for blade of aero-engine. *Proc Inst Mech Eng B J Eng Manuf* 2016;**230**:858–69.
105. Hahn RS. On the mechanics of the grinding process under plunge cut conditions. *J Manuf Sci Eng Trans Asme* 1966;**88**:72–9.
106. Zhu WL, Yang Y, Li HN, et al. Theoretical and experimental investigation of material removal mechanism in compliant shape adaptive grinding process. *Int J Mach Tools Manuf* 2019;**142**:76–97.
107. Cao JG, Nie M, Liu YM, et al. Ductile-brittle transition behavior in the ultrasonic vibration-assisted internal grinding of silicon carbide ceramics. *Int J Adv Manuf Technol* 2018;**96**:3251–62.
108. Gu XS, Zhao QL, Wang H, et al. Fundamental study on damage-free machining of sapphire: revealing damage mechanisms via combining elastic stress fields and crystallographic structure. *Ceram Int* 2019;**45**:20684–96.
109. Alfares M, Elsharkawy A. Effect of grinding forces on the vibration of grinding machine spindle system. *Int J Mach Tools Manuf* 2000;**40**:2003–30.
110. Badger J, Murphy S, O'Donnell G. The effect of wheel eccentricity and run-out on grinding forces, waviness, wheel wear and chatter. *Int J Mach Tools Manuf* 2011;**51**:766–74.
111. Chen JB, Fang QH, Li P. Effect of grinding wheel spindle vibration on surface roughness and subsurface damage in brittle material grinding. *Int J Mach Tools Manuf* 2015;**91**:12–23.
112. Zhou K, Ding HH, Zhang SY, et al. Modelling and simulation of the grinding force in rail grinding that considers the swing angle of the grinding stone. *Tribol Int* 2019;**137**:274–88.
113. Sun GY, Zhao LL, Ma Z, et al. Force prediction model considering material removal mechanism for axial ultrasonic vibration-assisted peripheral grinding of Zerodur. *Int J Adv Manuf Technol* 2018;**98**:2775–89.
114. Koshy P, Jain VK, Lal GK. Stochastic simulation approach to modelling diamond wheel topography. *Int J Mach Tools Manuf* 1997;**37**:751–61.
115. Jiang JL, Ge PQ, Hong J. Study on micro-interacting mechanism modeling in grinding process and ground surface roughness prediction. *Int J Adv Manuf Technol* 2013;**67**:1035–52.
116. Jiang JL, Ge PQ, Bi WB, et al. 2D/3D ground surface topography modeling considering dressing and wear effects in grinding process. *Int J Mach Tools Manuf* 2013;**74**:29–40.
117. Tamaki J, Kitagawa T. Evaluation of surface topography of metal-bonded diamond wheel utilizing three-dimensional profilometry. *Int J Mach Tools Manuf* 1995;**35**:1339–51.
118. Vairamuthu R, Bhushan BM, Srikanth R, et al. Performance enhancement of cylindrical grinding process with a portable diagnostic system. *Procedia Manuf* 2016;**5**:1320–36.
119. Inazaki I, Yonetsu S. Forced vibrations during surface grinding. *Jsme Int J Ser B Fluids Therm Eng* 1969;**12**:385–91.
120. Ding WF, Dai CW, Yu TY, et al. Grinding performance of textured monolayer CBN wheels: Undeformed chip thickness nonuniformity modeling and ground surface topography prediction. *Int J Mach Tools Manuf* 2017;**122**:66–80.
121. Myler HR, Weeks AR. *Computer imaging recipes in C*. New Jersey: Prentice-Hall; 1993.
122. He Z, Li JY, Liu YM, et al. Single-grain cutting based modeling of abrasive belt wear in cylindrical grinding. *Friction* 2020;**8**:208–20.
123. Wang Y, Fu ZQ, Dong YH, et al. Research on surface generating model in ultrasonic vibration-assisted grinding. *Int J Adv Manuf Technol* 2018;**96**:3429–36.
124. Miao Q, Ding WF, Xu JH, et al. Creep feed grinding induced gradient microstructures in the superficial layer of turbine blade root of single crystal nickel-based superalloy. *Int J Extreme Manuf* 2021;**3** 045102.
125. Ohmori H, Umezu S, Kim Y, et al. A high quality surface finish grinding process to produce total reflection mirror for x-ray fluorescence analysis. *Int J Extreme Manuf* 2020;**2** 015101.
126. Guo J, Goh MH, Wang P, et al. Investigation on surface integrity of electron beam melted Ti-6Al-4 V by precision grinding and electropolishing. *Chin J Aeronaut* 2021;**34**(12):28–38.
127. Cai R, Rowe WB. Assessment of vitrified CBN wheels for precision grinding. *Int J Mach Tools Manuf* 2004;**44**:1391–402.

128. Darafon A, Warkentin A, Bauer R. Characterization of grinding wheel topography using a white chromatic sensor. *Int J Mach Tools Manuf* 2013;**70**:22–31.
129. Hecker RL, Ramoneda IM, Liang SY. Analysis of wheel topography and grit force for grinding process modeling. *J Manuf Process* 2003;**5**:13–23.
130. Yu HY, Wang J, Lu YS. Modeling and analysis of dynamic cutting points density of the grinding wheel with an abrasive phyllotactic pattern. *Int J Adv Manuf Technol* 2016;**86**:1933–43.
131. Kaliszer H. Grinding technology. theory and applications of machining with abrasives. *Int J Mach Tools Manuf* 1991;**31**:435–6.
132. Kang MX, Zhang L, Tang WC. Study on three-dimensional topography modeling of the grinding wheel with image processing techniques. *Int J Mech Sci* 2020;**167** 105241.
133. Wu CJ, Dong WJ, Zhu LJ, et al. Modeling of grinding chip thickness distribution based on material removel mode in grinding of SiC ceramics. *J Adv Mech Des Syst* 2020;**14** JAMDSM0018.
134. Guo B, Zhao QL, Fang XY. Precision grinding of optical glass with laser micro-structured coarse-grained diamond wheels. *J Mater Process Technol* 2014;**214**:1045–51.
135. Chang HC, Wang JJJ. A stochastic grinding force model considering random grit distribution. *Int J Mach Tools Manuf* 2008;**48**:1335–44.
136. Chen Y, Chen X, Xu XP, et al. Quantitative impacts of regenerative vibration and abrasive wheel eccentricity on surface grinding dynamic performance. *Int J Adv Manuf Technol* 2018;**96**:2271–83.
137. Zhang T, Jiang F, Huang H, et al. Towards understanding the brittle-ductile transition in the extreme manufacturing. *Int J Extreme Manuf* 2021;**3** 022001.
138. Wang H, Pei ZJ, Cong WL. A mechanistic cutting force model based on ductile and brittle fracture material removal modes for edge surface grinding of CFRP composites using rotary ultrasonic machining. *Int J Mech Sci* 2020;**176** 105551.
139. Li HN, Yu TB, Wang ZX, et al. Detailed modeling of cutting forces in grinding process considering variable stages of grain-workpiece micro interactions. *Int J Mech Sci* 2017;**126**:319–39.
140. Wiercigroch M, Krivtsov A. Frictional chatter in orthogonal metal cutting. *Philos Trans Royal Soc Lond Ser A Math Phys Eng Sci* 2001;**359**:713–38.
141. Wu DW, Liu CR. An analytical model of cutting dynamics. part 1: model building. *J Manuf Sci Eng Trans Asme* 1985;**107**.
142. Davies MA, Burns TJ. Thermomechanical oscillations in material flow during high-speed machining. *Philos Trans Royal Soc Lond Ser A Math Phys Eng Sci* 2001;**359**:821–46.
143. Gradišek J, Govekar E, Grabec I. Chatter onset in non-regenerative cutting: a numerical study. *J Sound Vib* 2001;**242**:829–38.
144. Cho H, Corbi O, Khalil E, et al. Chaos in grinding process. *Wseas Trans Appl Theor Mech* 2009;**4**:195–204.
145. Liu Y, Zhao YL, Li JT, et al. Application of weighted contribution rate of nonlinear output frequency response functions to rotor rub-impact. *Mech Syst Signal Process* 2020;**136** 106518.
146. Leonesio M, Parenti P, Cassinari A, et al. Force-field instability in surface grinding. *Int J Adv Manuf Technol* 2014;**72**:1347–60.
147. Kurfess TR, Whitney DE, Brown ML. Verification of a dynamic grinding model. *J Dyn Syst Meas Control* 1988;**110**:403–9.
148. Jenkins HE, Kurfess TR, Ludwick SJ. Determination of a dynamic grinding model. *J Dyn Syst Meas Control Trans Asme* 1997;**119**:289–93.
149. Hahn RS. Controlled-force grinding—a new technique for precision internal grinding. *J Manuf Sci Eng Trans Asme* 1964;**86** 287.
150. Zhao H, Zhu LM, Ding H. A parametric interpolator with minimal feed fluctuation for CNC machine tools using arc-length compensation and feedback correction. *Int J Mach Tools Manuf* 2013;**75**:1–8.
151. Hu W, Yang W, Xiong Y. An adaptive mesh model for 3D reconstruction from unorganized data points. *Int J Adv Manuf Technol* 2005;**26**:1362–9.
152. Chen ST, Jiang ZH. A force controlled grinding-milling technique for quartz-glass micromachining. *J Mater Process Technol* 2015;**216**:206–15.
153. Jackson MJ. Recent advances in ultraprecision abrasive machining processes. *SN Appl Sci* 2020;**2**:1172.
154. Wang QR, Lin S, Jiang ZH, et al. Fewer-axis grinding methodology with simultaneously guaranteeing surface accuracy and grinding force for large optical SiC mirror. *Int J Adv Manuf Technol* 2018;**99**:1863–75.
155. Tönshoff HK, Zinngrebe M, Kemmerling M. Optimization of internal grinding by microcomputer-based force control. *CIRP Ann* 1986;**35**:293–6.
156. Guo L, Schone A, Ding X. Grinding force control using nonlinear adaptive strategy. *Automat Control - World Congr* 1993;**5**:459–62.
157. Chen ST, Chen YY. Microgroove grinding of monocrystalline diamond using medium-frequency vibration-assisted grinding with self-sensing grinding force technique. *J Mater Process Technol* 2020;**282** 116686.
158. Rowe WB. Thermal analysis of high efficiency deep grinding. *Int J Mach Tools Manuf* 2001;**41**:1–19.
159. Liu Y, Xu JY, Xiao GJ, et al. Thermo-mechanical coupling during belt grinding and corresponding surface integrity of titanium alloy. *Int J Adv Manuf Technol* 2022;**121**:6599–609.
160. Park HW, Liang SY. Force modeling of microscale grinding process incorporating thermal effects. *Int J Adv Manuf Technol* 2009;**44**:476–86.
161. Naskar A, Choudhary A, Paul S. Wear mechanism in high-speed superabrasive grinding of titanium alloy and its effect on surface integrity. *Wear* 2020;**462** 203475.
162. Huang XM, Ren YH, Wu W, et al. Research on grind-hardening layer and residual stresses based on variable grinding forces. *Int J Adv Manuf Technol* 2019;**103**:1045–55.
163. Yao CF, Wang T, Xiao W, et al. Experimental study on grinding force and grinding temperature of Aermet 100 steel in surface grinding. *J Mater Process Technol* 2014;**214**:2191–9.
164. Dargusch MS, Sivarupan T, Bermingham M, et al. Challenges in laser-assisted milling of titanium alloys. *Int J Extreme Manuf* 2021;**3** 015001.
165. Guo B, Zhao QL. Ultrasonic vibration assisted grinding of hard and brittle linear micro-structured surfaces. *Precis Eng J Int Soc Precis Eng Nanotechnol* 2017;**48**:98–106.